Cholesterol metabolism in mouse models of atherosclerosis and adrenal steroidogenesis

Sluis, R.J. van der

3

HDL IS ESSENTIAL FOR ATHEROSCLEROTIC LESION REGRESSION IN APOE KNOCKOUT MICE BY BONE MARROW APOE RECONSTITUTION

Ronald J. van der Sluis, Robin A.F. Verwilligen, Zsuzsanna Lendvai,
Robbert Wever, Menno Hoekstra, Miranda van Eck

ABSTRACT

BACKGROUND AND AIM: Although studies in mice have suggested that lesion regression is feasible, the underlying mechanisms remain largely unknown. Here we determined the impact of high-density lipoprotein (HDL) on atherosclerosis regression outcome.

METHODS: Atherosclerotic lesion dynamics were studied upon bone marrow transplantation-mediated re-introduction of apolipoprotein E (ApoE) in ApoE knockout mice. Probucol was used to pharmacologically deplete HDL.

RESULTS: Restoration of ApoE function was associated with an initial growth of atherosclerotic lesions and parallel decrease in lesional macrophage foam cell content (47 ± 4 % at 4 weeks versus 72 ± 2 % at baseline: $P<0.001$), despite the fact that cholesterol levels were markedly reduced. Notably, significant lesion regression was detected from 4 weeks onwards, when plasma cholesterol levels had returned to the normolipidemic range. As a result, lesions were 41 % smaller ($P<0.05$) at 8 weeks than at 4 weeks after bone marrow transplantation. Regressed lesions contained an even lower level of macrophage foam cells (33 ± 5 %: $P<0.001$) and were rich in collagen. Probucol co-treatment was associated with a 3.2-fold lower ($P<0.05$) plasma HDL-cholesterol level and a more pro-inflammatory (C-C chemokine receptor type 2: CCR2+) monocyte phenotype. Importantly, probucol-treated mice exhibited atherosclerotic lesions that were larger than those of regular chow diet-fed bone marrow transplanted mice at 8 weeks (186 ± $15*10^3$ μm^2 for probucol-treated versus 120 ± $19*10^3$ μm^2 for controls: $P<0.05$).

CONCLUSIONS: We have shown that probucol-induced HDL deficiency impairs the ability of established lesions to regress in response to reversal of the genetic hypercholesterolemia in ApoE knockout mice. Our studies thus highlight a crucial role for HDL in the process of atherosclerosis regression.

INTRODUCTION

Atherosclerosis is the primary underlying cause of cardiovascular disease morbidity and mortality [1]. Accumulation of cholesterol within macrophages (foam cell formation) as a result of chronic hypercholesterolemia is a hallmark in the development of atherosclerotic lesions. Despite effective lipid-lowering therapies to inhibit the generation of macrophage foam cells and the progression of atherosclerotic lesions, the worldwide incidence of cardiovascular disease remains high. In order to further reduce cardiovascular disease-related mortality and morbidity, inducing regression of established atherosclerotic lesions is considered an important therapeutic challenge. Human trials have shown that regression of existing lesions is possible under intensive lipid lowering conditions. However, the extent of lesion regression achieved with current drug treatments is limited (change in mean percentage atheroma volume: 0.7 to 1.76 %) [2-4]

Despite the fact that only small reductions in lesion size have thus far been observed in the human setting, it has become evident from mouse models that regression of lesions is feasible, i.e. under extreme lipid lowering conditions [5]. Notably, the mechanisms underlying the lesion regression observed in animal models are still subject of debate. Studies by the groups of Ed Fisher and Steve Young have suggested that macrophage emigration from the lesions is the driving force behind lesion regression. More specifically, they showed that acute elimination of hypercholesterolemia through either timed inactivation of the microsomal triglyceride transfer protein gene, i.e. in the so-called Reversa mice, or via transplantation of an atherosclerotic lesion-containing vessel into a normolipidemic wild-type mouse is able to induce a significant decline in the atherosclerotic lesion size [6-8]. In sharp contrast to the macrophage emigration hypothesis, studies in which the hypercholesterolemia in ApoE knockout mice was reversed through adenovirus-mediated reconstruction of ApoE have suggested that impaired recruitment of new monocytes and macrophage apoptosis together actually facilitate the disappearance of macrophages from established lesions [9-12]. Since the mechanism underlying lesion regression could theoretically be dependent on the animal model used, we have recently developed an additional regression mouse model that may aid in uncovering the biological pathways that contribute to lesion regression. Hereto, we used bone marrow transplantation to reintroduce ApoE in ApoE knockout mice and reverse hypercholesterolemia and induce lesion regression [13].

We hypothesize that ApoE-mediated lowering of pro-atherogenic plasma very-low-density lipoprotein (VLDL) and low-density lipoprotein (LDL)-cholesterol levels opens up the possibility for macrophage foam cells to unload, i.e. efflux their excess cholesterol to anti-atherogenic high-density lipoprotein (HDL) for subsequent reverse cholesterol transport and initiation of lesion regression [14,15]. Feig et al., already showed with the aorta transplantation model that the presence of HDL-cholesterol is of importance for the emigration of CD68+ macrophages from atherosclerotic lesions [14]. In the current study we aimed to provide additional experimental support for the hypothesis that regression of atherosclerotic lesions requires restoration of macrophage cholesterol homeostasis by reducing the influx of pro-atherogenic lipoproteins in the presence of functional cellular cholesterol efflux pathways. Hereto, we investigated (1) the atherosclerotic lesion dynamics upon bone marrow transplantation-mediated re-introduction of ApoE in ApoE knockout mice and (2) the impact of pharmacological HDL depletion on atherosclerosis regression outcome.

MATERIALS AND METHODS

IN VIVO SETUP

Animal experiments were performed in a temperature and light cycle (12 hour light: 12 hour darkness) controlled room at the Gorlaeus Laboratories of Leiden University, where the Leiden Academic Centre for Drug Research is located. All animal work was approved by the Dutch Ethics Committee and regulatory authority at Leiden University and was carried out in compliance with Dutch government guidelines and the Directive 2010/63/EU of the European Parliament on the protection of animals used for scientific purposes.

The data presented in this manuscript were derived from two independent experiments, one experiment in which we studied the lesion dynamics over time and a second study that involved the effect of probucol-induced HDL lowering on overall lesion regression outcome. In both experiments, 14-week old, in house bred, age-matched homozygous female ApoE knockout mice (C57BL/6 background) were used. At baseline, a group of 12 mice was sacrificed to determine the initial extent of lesion formation. The remaining mice were subjected to bone marrow transplantation with the aim to reverse the hypercholesterolemia. Prior to the bone marrow transplantation, bone marrow recipient mice received a 2 x 4.5 Gy X-ray total-body irradiation (0.19 Gy/min, 200KV, 4 mA) using an Andrex smart 225 Röntgen source (YXLON international).

Bone marrow from the tibias and femurs of in house bred normolipidemic C57BL/6 female donor mice was harvested, filtered to create an unicellular suspension and counted. A total amount of $5*10^6$ bone marrow cells was intravenously injected into the tail vain of the irradiated recipient mice. Throughout the bone marrow transplantation experiments, all mice were housed in individual ventilation cages and received chow diet (RM3 (E) DU: Special Diet Services, Witham, England) with or without probucol supplementation (0.025 % w/w: MP Biomedicals, Santa Ana, USA) and autoclaved water supplemented with antibiotics (83 mg/L Ciprofloxacin, 67 mg/L Polymyxin B sulfate, 6.5 g/L Sucrose) ad libitum. Mice were sacrificed at 2 and 4 weeks post transplantation in the timeline experiment and at 8 weeks post bone marrow transplantation in the probucol experiment. The data from the baseline groups of the two studies were pooled. Data from the experimental group of the probucol study that received a regular chow diet served as the 8 week data point in the timeline analysis.

At the day of sacrifice, mice were anesthetized with a mix of Xylazine (70 mg/kg), Ketamine (350 mg/kg) and Atropine (1.8 mg/kg) prior to in situ perfusion with phosphate buffered saline (pressure 100 mmHg) for 10 min via a cannula in the left ventricular apex. Organs (liver, spleen, adrenals) were harvested and stored for 24 h in 3.7 % formalin (Formal-fixx®, Shandon Scientific Ltd., UK) for tissue sectioning and further analysis.

PLASMA ANALYSES

Throughout both studies, tail vein blood from each individual mouse was obtained and collected in EDTA-coated tubes (Sarstedt, Numbrecht, Germany) for quantification of plasma lipids. Free cholesterol (FC) was determined by using an enzymatic colorimetric assay with 0.048 U/mL cholesterol oxidase (Calbiochem, San Diego, CA, USA) and 0.065 U/mL peroxidase (Sigma-Aldrich, Steinheim, Germany) in reaction buffer (1.0 KPi buffer, pH = 7.7 containing 0.01 M phenol, 1 mM 4-amino-antipyrine, 1 % polyoxyethylene-9-laurylether, and 7.5 % methanol). For the determination of total cholesterol (TC), 0.03 U/mL cholesteryl esterase (Calbiochem, San Diego, CA, USA) was added to the reaction solution. Absorbance was read at 490 nm on a Powerwave 340 from BioTek. Lipoproteins in pooled plasma were separated by means of fast protein liquid chromatography (FPLC: Superose 6 column: 3.2 x 30 mm: Smart-System, Pharmacia, Uppsala, Sweden) and the cholesterol content was analyzed as described above. Fractions 1-13 represented the non-HDL species VLDL and LDL and fractions 13-19 represented HDL. Corticosterone levels were determined in 1:200 diluted EDTA-plasma from orbital vein blood collected at sacrifice using a ^{125}I-corticosterone kit (MP Biomedicals, Santa Ana, USA) following the manufacturer's protocol.

BLOOD CELL ANALYSIS

Routine whole blood cell analysis was performed using the automated Sysmex XT-2000iV Veterinary Haematology analyzer (Sysmex Corporation) on endpoint orbital vein blood, collected in EDTA-coated tubes (Sarstedt, Numbrecht, Germany). To identify specific blood cell subsets, orbital vein blood was subjected to flow cytometric analysis. Hereto, orbital vein blood was isolated and red blood cells were removed using an ACK lysis buffer (0.15 M NH_4Cl, 1 mM $KHCO_3$, 0.1 mM Na_2EDTA, pH = 7.3). The leukocyte fractions were stained with the following antibodies: CD4-PerCP (clone RM4-5: BD Biosciences), CD8-APC (clone 53-6.7: eBioscience), Ly6G-FITC (clone 1A8: eBioscience), Ly6C-PE (clone HK1.4: eBioscience). Flow cytometry was performed on a FACS Canto II (Becton Dickinson, Mountain View, CA, US). Data were analyzed using FACS DIVA software (BD Biosciences).

ANALYSIS OF GENE EXPRESSION BY REAL-TIME QUANTITATIVE PCR

Quantitative gene expression analysis was performed as previously described [16]. In brief, total RNA was isolated using a standard phenol/chloroform extraction method and reverse transcribed using RevertAid Reverse Transcriptase. Gene expression analysis was performed using SYBR-Green technology (Eurogentec) on a 7500 Fast Real time PCR system (Applied Biosystems, Foster city, US). Primers were validated for an equal efficiency. Ratios of the target gene expression were determined by subtracting the Ct of the target gene from the average Ct of the housekeeping genes and raised by 2 to the power of this difference. Glyceraldehyde 3-phosphate dehydrogenase (GAPDH), ribosomal protein lateral stalk subunit P0 (36b4) and beta-actin (β-actin) were used as the housekeeping genes. General information of the primers used is summarized in **Table 1**.

Table 1: Primers used for QPCR analysis.

Name	Ref Seq (mRNA)	Primer Forward	Primer Reverse
36B4	NM_007475	5′-CTGAGTACACCTTCCCACTTACTGA-3′	5′-CGACTCTTCCTTTGCTTCAGCTTT-3′
B-ACTIN	NM_007393	5′-AACCGTGAAAAGATGACCCAGAT-3′	5′-CACAGCCTGGATGGCTACGTA-3′
GAPDH	NM_008084	5′-ATCCTGCACCACCAACTGCTTA-3′	5′-CATCACGCCACAGCTTTCCAG-3′
CD68	NM_001291058	5′-TGCCTGACAAGGGACACTTCGGG-3′	5′-GCGGGTGATGCAGAAGGCGATG-3′
ApoE	NM_009696	5′-CCGTGCTGTTGGTCACATTGC-3′	5′-AGCGCAGGTAATCCCAGAAGC-3′

HISTOLOGICAL ANALYSIS

Atherosclerotic lesion quantification was performed in the aortic root. Hereto, 10 µm cryostat sections (Leica CM 350S cryostat) were collected from OCT compound (Tissue-Tek, Sakura Finetek, Alphen a/d Rijn, The Netherlands) embedded hearts starting at the appearance of the aortic valves up to 300 µm into the ascending aorta. Sections were stained for neutral lipids with Oil red O and counterstained with hematoxylin (Sigma-Aldrich, Steinheim, Germany). Collagen was visualized by a Masson's trichrome staining (Sigma-Aldrich, Steinheim, Germany) according to the manufacturer's instructions. Lesional foam cell content was determined based on their foamy appearance in the Masson's Trichrome stained atherosclerotic lesions. Blinded quantification of each staining was performed on 5 sections per mouse using Leica Qwin Imaging software (Leica Ltd., Cambridge, UK). Adrenal morphology and lipid content were examined on 10 µm cryostat sections embedded in OCT compound. A hematoxylin-eosin staining was performed for general morphology and the neutral lipid content was visualized using an Oil red O staining.

IN VITRO MACROPHAGE CHOLESTEROL EFFLUX

To obtain peritoneal macrophages for in vitro cholesterol efflux experiments, C57BL/6 mice were injected intraperitoneally with 1 ml 3 % Brewer's thioglycollate medium. At 5 days after injection, the peritoneal cavity of the mice was lavaged with 10 ml cold PBS to collect thioglycollate-elicited peritoneal macrophages [17]. Thioglycollate-elicited peritoneal macrophages were cultured overnight in DMEM containing 10 % fetal calf serum for optimal adherence. Subsequently, the fetal calf serum was removed and cells were washed with PBS. Next, the cells were exposed to 0.5 µCi [^{3}H]-cholesterol (Perkin Elmer, Waltham, MA, US) in DMEM with 0.2 % fatty acid free BSA which was removed after 24 h. The ability of the macrophages to efflux the incorporated radioactive cholesterol towards plasma lipoproteins, i.e. HDL, was then studied by incubation with 2.5 % (v/v) plasma of ApoE knockout mice transplanted with wild-type bone marrow fed the chow diet with or without probucol supplementation. Cholesterol efflux was measured after 4 h and calculated as the percentage of radioactivity in the medium compared with the total amount of radioactivity in the medium and cells.

STATISTICAL ANALYSES

Statistical analysis was performed using GraphPad Instat Software (San Diego, CA, USA, http://www.graphpad.com). Normality testing was performed using the method of Kolmogorov and Smirnov. Significance was calculated using a two-tailed Student's t-test or two-way ANOVA with Bonferroni's post-test where appropriate. $P<0.05$ was considered significant.

RESULTS

To provide more insight into the dynamics of atherosclerosis regression, we monitored the impact of reversal of the genetic hypercholesterolemia on atherosclerotic lesion size and composition in ApoE knockout mice over time. Hereto, ApoE-containing C57BL/6 wild-type bone marrow was transplanted into lethally irradiated 14-week old ApoE knockout mice with macrophage foam cell-rich early lesions.
ApoE mRNA expression was measured in liver specimens to verify bone marrow transplantation-induced repopulation of hepatic ApoE-expressing macrophages (Kupffer cells) at 8 weeks after transplantation. No functional ApoE mRNA could be detected in the baseline group of mice sacrificed before bone marrow transplantation. However, in line with an effective repopulation of bone marrow-derived cells, a gradual increase in hepatic ApoE expression could be observed over time in mice transplanted with C57BL/6 wild-type bone marrow (**Figure 1A**).

The restored hepatic uptake of VLDL particles upon re-constitution of ApoE production by bone marrow-derived cells in ApoE knockout mice [18] was associated with a time-dependent decline in plasma total cholesterol levels. As can be appreciated from **Figure 1B**, total cholesterol levels were 2-fold lowered ($P<0.001$) at 2 weeks after bone marrow transplantation and reached wild type normolipidemic values of ≤100 mg/dL [19] already at the 4 week time point. Plasma cholesterol levels continued to decrease, translating in a 5.8-fold lowering ($P<0.001$) as compared to baseline levels at 8 weeks after bone marrow transplantation. In contrast, no change in plasma triglycerides (TG) was observed during the course of the study (**Figure 1C**). Lipoprotein distribution analysis validated that the observed decrease in plasma total cholesterol levels could be attributed to a decrease in VLDL/LDL (non-HDL)-cholesterol levels (**Figure 1D**).

Infiltration of monocytes into the arterial wall where they are converted into macrophages and become foam cells is a hallmark of atherosclerosis development. Hence monocyte counts are an important predictor of atherosclerosis susceptibility [20]. Blood specimens collected at each time point were subject to routine hematological analysis to uncover a potential effect of the bone marrow transplantation procedure and the lipid lowering on blood cell composition. In accordance with the notion that proliferating cells are highly susceptible to irradiation-induced death, a clear trend towards a deprivation of blood lymphocytes could be observed at 2 weeks after bone marrow transplantation ($3.54 \pm 0.17*10^9$/L for baseline versus $1.41 \pm 0.19*10^9$/L for T = 2w: P=0.18: **Figure 1E**). The initial decrease in blood lymphocyte concentrations

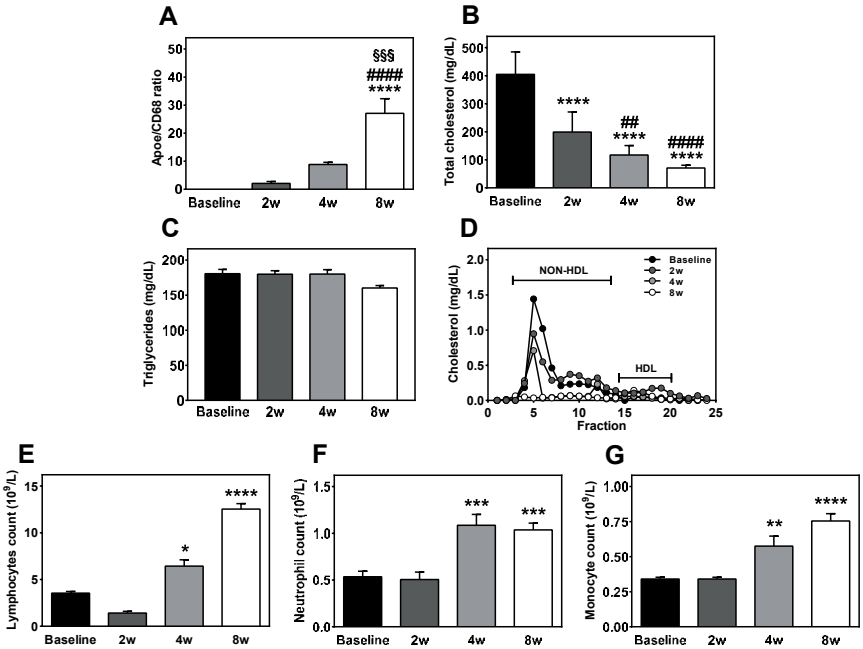

Figure 1: Bone marrow transplantation-induced reconstitution of ApoE in ApoE knockout mice increased hepatic ApoE expression levels over time (A), lowered plasma total cholesterol levels (B), did not change triglyceride levels over time (C), depleted the non-HDL fraction (D) and was associated with a time-dependent effect on blood leukocyte counts (E, F, G). All data represent means+SEM with baseline n=24, T = 2w n=12, T = 4w n=13, T = 8w n=10. *P<0.05, **P<0.01, ***P<0.005, ****P<0.001 vs. baseline: ##P<0.01, ###P<0.005 vs. T = 2w: $$$P<0.005 vs. T = 4w.

was followed by a full restoration at 4 weeks and a marked overshoot at 8 weeks after transplantation (T = 8w: 12.54 ± 0.57*10^9/L: P<0.001 versus baseline). No irradiation-associated decrease in blood neutrophil or monocyte levels was noted in the 2 weeks after the bone marrow transplantation, probably due to the fact that these immune cells are relatively resistant to irradiation damage. Blood counts of these latter two cell types were actually increased from 4 weeks onwards in wild-type bone marrow transplanted ApoE knockout mice as compared to those in ApoE knockout mice at baseline (**Figure 1F and G**).

The extent of atherosclerosis in the different groups of mice was quantified in the aortic root. At baseline, ApoE knockout mice exhibited atherosclerotic lesions of 98 ± 10*10^3 μm^2 that were rich in macrophage foam cells (**Figure 2A and B**). Despite the fact that cholesterol levels were already significantly reduced at 2 weeks after bone

marrow transplantation, significant growth of the atherosclerotic lesions was observed, reaching a size of 202 ± 14*10^3 μm^2 at 4 weeks post bone marrow transplantation ($P<0.005$). Lesion composition analysis indicated that the increase in size was paralleled by a significant decrease in the foam cell core in the 4 weeks after bone marrow ApoE reconstitution (**Figure 2B**). Lesional collagen content was not affected during the lesion progression (**Figure 2C**), but the relative necrotic area was doubled ($P<0.01$: **Figure 2D**). Importantly, as can be appreciated from **Figure 2A**, the initial progression of the lesions up to 4 weeks after ApoE re-introduction was followed by significant lesion regression during the following 4 weeks. As such, the average size of the atherosclerotic lesions at 8 weeks after bone marrow transplantation was 41% smaller ($P<0.05$) than that at 4 weeks post bone marrow transplantation and not significantly different from that at baseline. The relative contribution of macrophage foam cells to total lesion area was even further decreased during the lesion regression phase to 33 ± 5 % at 8 weeks after transplantation (**Figure 2B**). Notably, the collagen content was 1.4-fold higher in regressing lesions (T = 8w) as compared to lesions in the progression phase (T = 4w) (**Figure 2C**). It thus appears that atherosclerosis regression is associated with a switch from a highly cellular (foam cell-rich) lesion towards a more acellular (collagen-rich) lesion phenotype. When taking the blood cholesterol levels and lesion dynamics profile into account, it can be suggested that lesion regression, as defined by a decrease in lesion size, initiates when plasma cholesterol levels are decreased to those found in normolipidemic wild-type mice (≤100 mg/dL).

Apolipoprotein A1 (ApoA1)-containing HDL, through interaction with the membrane proteins ATP-binding cassette transporter A1 (ABCA1) and G1 (ABCG1) and scavenger receptor BI (SR-BI) can acquire excess cholesterol from macrophage foam cells for subsequent transport to and excretion by the liver [21]. The lipid-lowering drug probucol is a potent inhibitor of ABCA1-mediated cholesterol efflux as it interferes with cellular ApoA1 binding [22] and lowers the availability of ABCA1 on the membrane [23]. As such, in vivo probucol treatment is associated with an impairment of ABCA1-mediated lipidation of HDL particles and functional HDL deficiency [24-26]. To show the effect of pharmacological reduction of HDL by probucol treatment on lesion regression, a transplantation of wild-type bone marrow into ApoE knockout mice was combined with administration of probucol (0.25 % w/w) via the chow diet.

As demonstrated in **Figure 3A**, probucol treatment did not change the ability of bone marrow cell-derived ApoE to reverse the genetic hypercholesterolemia. Cholesterol levels decreased rapidly upon transplantation with wild-type bone marrow in both

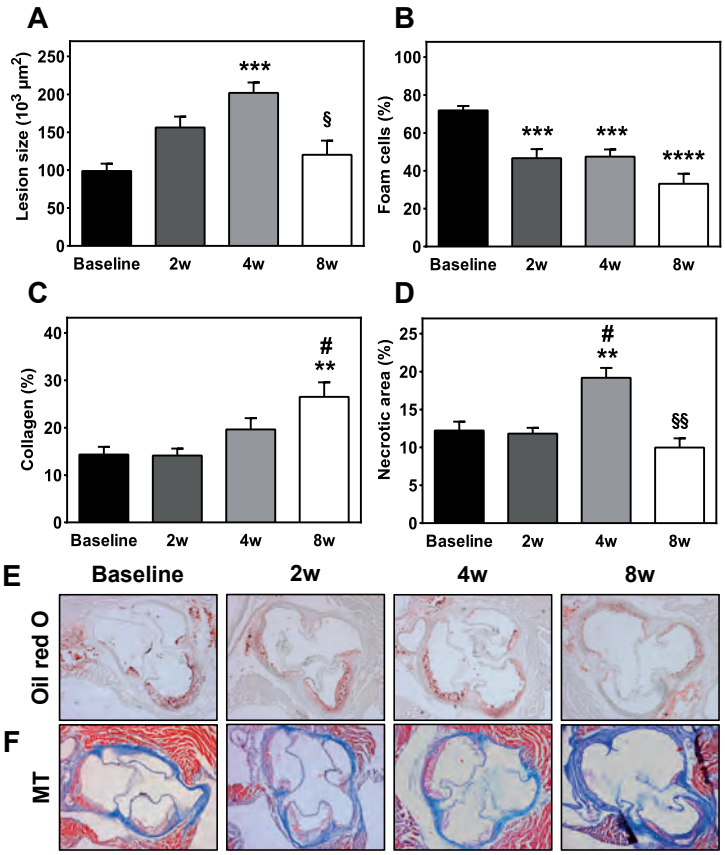

Figure 2: Bone marrow transplantation-induced reconstitution of ApoE in ApoE knockout mice was associated with lesion progression followed by lesion regression (A), a gradual decrease in lesional macrophage foam cell content (B), an increase in lesional collagen content (C), and a time-dependent increase in lesional necrotic core size (D). Representative pictures of Oil red O and Masson's trichrome (MT)-stained aortic root sections used for the quantification of the composition are shown in panels E and F (original magnification 5X). Data represent means + SEM with baseline n=24, T = 2w n=12, T = 4w n=13, T = 8w n=10, **P<0.01, ***P<0.005, ****P<0.001 vs. baseline: #P<0.05 vs. T = 2w: §P<0.05, §§P<0.01 vs. T = 4w.

treatment groups, as expected. However, plasma total cholesterol levels were consistently lower in probucol-treated mice as compared to regular chow diet-fed mice. FPLC-based lipoprotein fractionation performed at sacrifice -8 weeks after bone marrow transplantation - confirmed that the decrease in plasma total cholesterol levels could be attributed to the probucol-induced HDL deficiency (**Figure 3B**). HDL-cholesterol levels were 3.2-fold lower (P<0.001) in probucol-treated mice as compared

to controls. In accordance with the notion that the decrease in HDL levels impairs the ability to induce cholesterol efflux from macrophages, the extent of [^{3}H]-cholesterol efflux from wild-type macrophages to plasma from probucol-treated mice was significantly lower than that to plasma from non-supplemented chow diet-fed mice (10.6 ± 0.8 % for probucol versus 17.2 ± 0.8 % for control: P<0.001: Figure 3C). Our previous studies have suggested that, in normolipidemic C57Bl/6 mice, HDL, via an interaction with SR-BI, delivers the cholesterol substrate for glucocorticoid production to the

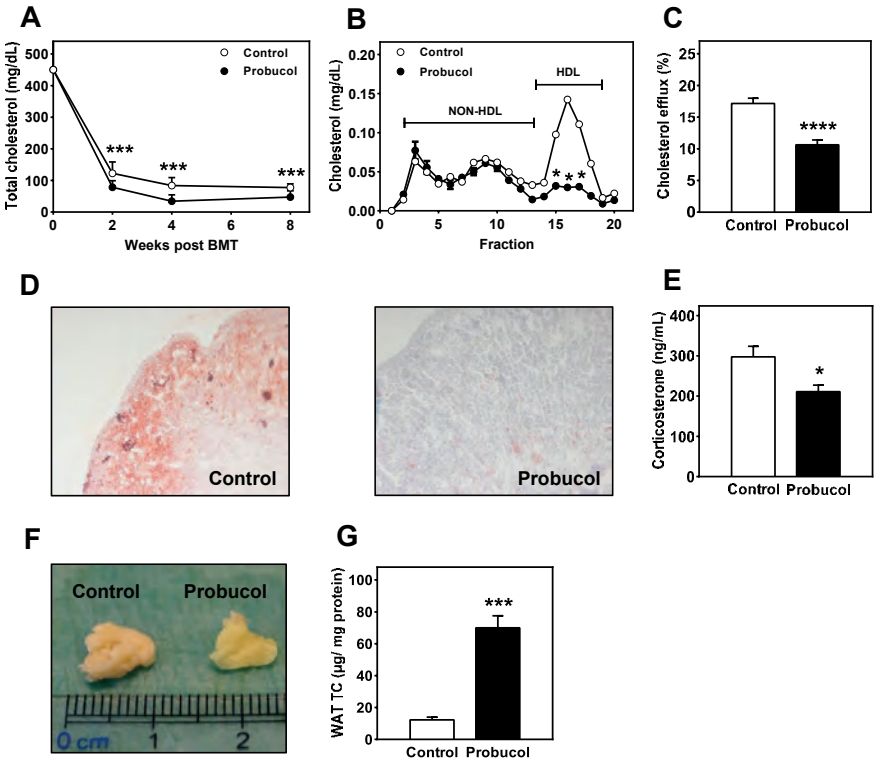

Figure 3: Probucol treatment in ApoE knockout mice transplanted with ApoE-containing bone marrow resulted in a decrease in plasma cholesterol levels (A), which could be attributed to HDL depletion (B: 8 week time point). Plasma from probucol-fed mice as compared to regular chow diet-fed mice exhibits a diminished capacity to induce cholesterol efflux from cultured C57BL/6 wild-type macrophages (C). Probucol supplemented diet feeding is associated with adrenal neutral lipid depletion as compared to control chow diet feeding (D)(original magnification 5X) and a decrease in plasma corticosterone levels (E). Probucol treatment is associated with a yellowish appearance of white adipose tissue (F) and an increase in white adipose tissue total cholesterol levels (G). All data represent means+SEM with control n=10 and probucol n=7. *P<0.05, ***P<0.005, ****P<0.001 vs. control.

adrenals [27]. Histological examination of adrenal sections revealed that control mice displayed neutral lipid positive areas within the adrenal cortex, while this was absent in probucol-fed mice (**Figure 3D**). In addition, levels of the primary glucocorticoid species corticosterone were 29 % lower in sacrifice plasma from probucol-fed mice ($P<0.05$: **Figure 3E**). Probucol treatment thus not only diminished the plasma cholesterol efflux capacity but also effectively impaired HDL's function in the delivery of cholesterol to the adrenals. Interestingly, during sacrifice, it was noted that the white adipose tissue of probucol-treated mice exhibited a yellowish appearance (**Figure 3F**).

Krinsky et al. [28] have shown that HDL has the capacity to take up and transport carotenoids, a colored pigment anti-oxidant As such, HDL depletion could induce an accumulation of carotenoids in organs like white adipose tissue. Given that probucol is a highly lipophilic substance, it is anticipated that probucol itself also accumulated in fat tissue. The yellowish appearance can thus also be the result of the accumulation of probucol catabolites that appear green/yellowish [23,29]. In support of probucol storage and the associated inhibition of ABCA1 functionality and cholesterol efflux from adipocytes, we observed that the cholesterol content was markedly higher (6-fold: $P<0.005$) in adipose tissue of probucol-treated mice as compared to that of regular chow diet-fed controls (**Figure 3G**).

In addition to HDL anti-atherogenic role in cholesterol efflux, HDL can also directly impact on the pro-atherogenic immune function of monocytes. More specifically, Han et al. have shown that exposure of HDL to monocytes in vitro lowers the expression of the C-C chemokine receptor type 2 (CCR2), leading to a reduced monocyte migration towards the pro-inflammatory cytokine CCL2/MCP-1 [30]. Monocyte numbers in the blood circulation were not changed by probucol exposure (**Figure 4A**). However, in further support of the induction of functional HDL deficiency upon probucol treatment, the fraction of the circulating monocytes expressing CCR2 was significantly higher in probucol-treated mice (61 ± 2 % for probucol-treated mice versus 47 ± 2 % for control mice: $P<0.005$: **Figure 4B**). As indicated by Swirski et al., the spleen acts as a reservoir for CCR2+ monocytes [31]. In line with the change in the circulating monocyte profile, probucol-treated mice displayed an increased splenic size (data not shown).

Next, the primary readout of our experiment was analyzed, the effects on atherosclerotic lesion regression. At 8 weeks after ApoE re-introduction, atherosclerotic lesions in both groups of mice were low in macrophage foam cell numbers (**Figure 5B**) and contained an equally large necrotic core area (**Figure 5C**). Interestingly, lowering HDL resulted in

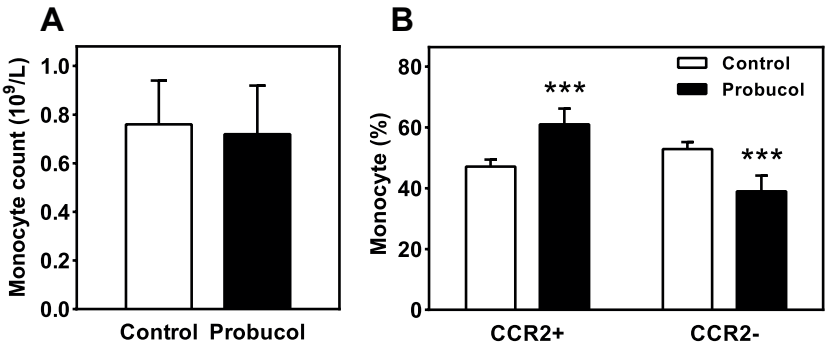

Figure 4: Probucol-induced HDL lowering did not change blood monocyte counts in ApoE knockout mice reconstituted with ApoE-positive bone marrow (A), but did increase the relative fraction of monocytes carrying CCR2 (B). Data represents means+SEM with control n=10 and probucol n=7 mice. ***P<0.005 vs. control.

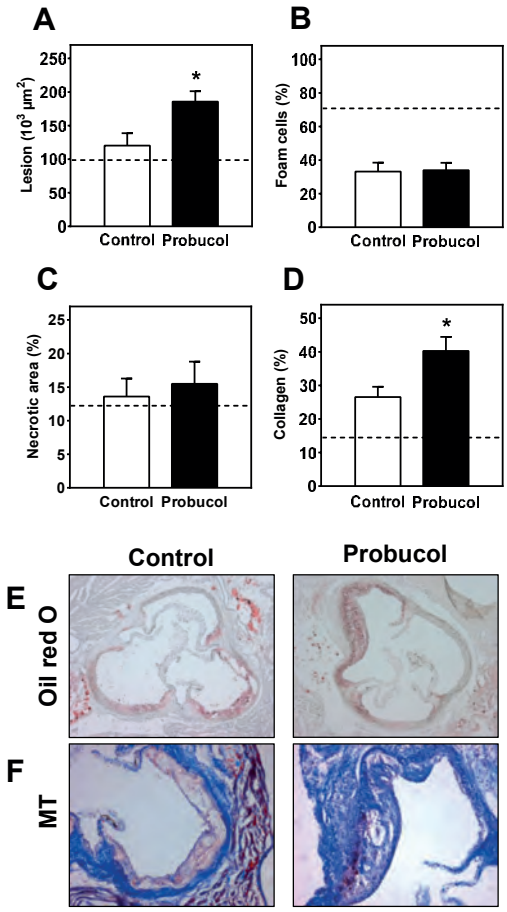

Figure 5: Probucol treatment was associated with larger atherosclerotic lesions versus control at 8 weeks post reconstitution of ApoE-positive bone marrow into ApoE knockout mice (A) an unchanged lesion macrophage foam cell and necrotic area content (B & C) and an enlarged collagen content (D). Data represent means +SEM with control n=10 and probucol n=7. *P<0.05 vs. control. Representative photomicrographs of Oil red O-stained and Masson's Trichrome (MT)-stained aortic root lesions are shown in panels E and F (original magnification Oil Red O: 5X and MT: 10X, respectively).

an increase in the amount of collagen in the lesions (**Figure 5D**). Importantly, as evident from **Figure 5A**, probucol-treated mice exhibited atherosclerotic lesions that were significantly larger than those of regular chow diet-fed bone marrow transplanted mice ($186 \pm 15*10^3 \mu m^2$ for probucol-treated mice versus $120 \pm 19*10^3 \mu m^2$ for control mice: $P<0.05$). The changes in plasma HDL-cholesterol levels, cholesterol efflux capacity, glucocorticoid output and inflammation status in response to probucol treatment were thus apparently accompanied by a marked impairment in the ability of aortic root atherosclerotic lesions to regress.

DISCUSSION

Here we aimed to provide proof for the hypothesis that HDL is essential for the regression of established atherosclerotic lesions observed in response to re-introduction of ApoE in ApoE knockout mice through bone marrow transplantation. The key findings of the current study are that, in our experimental mouse model, regression of existing lesions is initiated when plasma cholesterol levels are lowered to those within the normolipidemic range (<100 ng/mL) and that probucol-induced depletion of HDL impairs the ability of established lesions to regress.

We validated our previous findings that bone marrow transplantation-induced reversal of hypercholesterolemia in ApoE knockout mice is associated with a decrease in lesional macrophage foam cell content [13]. Our lesion dynamics analysis indicated that the initial decrease in macrophage foam cell content became evident as early as 2 weeks after bone marrow transplantation. In line, Feig et al. showed, using the Reversa mice, a gradual decrease in plaque macrophage content up till 4 weeks after the induction of lesion regression [8]. Studies using adenovirus-mediated replenishment of ApoE in ApoE knockout mice have suggested that the decrease in plaque macrophage content in response to lipid lowering can be attributed to a decrease in monocyte infiltration into the lesions in the context of an unchanged macrophage apoptosis rate [9]. Similarly to our findings, Potteaux et al. did not detect a decrease in absolute blood monocyte numbers upon ApoE re-introduction [9]. The decrease in monocyte infiltration observed in the study of Potteaux et al. appeared to be driven by a change in monocyte activation status. Using flow cytometry we could verify the observation of Potteaux et al. that lipid lowering does not change the ratio between $LyC6^{high}$ and $LyC6^{low}$ monocytes (data not shown). Unfortunately, we did not include in our flow cytometry panel the monocyte activation marker CD62L that was changed in the Potteaux study. As such, we cannot not exclude that the monocyte

activation status was changed after bone marrow transplantation-mediated ApoE re-introduction. However, given that (1) cholesterol lowering preceded the inhibition of monocyte recruitment into plaques in the ApoE adenovirus studies by Potteaux et al. and (2) our ApoE knockout mice still displayed significant hypercholesterolemia at 2 weeks after bone marrow transplantation and actually showed lesion progression, we anticipate that the initial decrease in plaque cellularity is not driven by a change in the monocyte infiltration rate. In our experimental setup we subjected the mice to total body irradiation to be able to efficiently transplant ApoE-containing wild-type bone marrow and thereby lower plasma cholesterol levels. Studies by Lorimore et al. have indicated that macrophages become activated and display secondary necrosis as a bystander effect in whole body irradiation-induced tissue damage in vivo [32]. It is therefore suggested that the decrease in lesional cellular content / macrophages in the initial (lesion progression) stage is rather due to irradiation-related necrosis and not primarily the result of a change in the lipid environment.

Given the relatively long time between the irradiation and the start of atherosclerosis regression (>4 weeks), other mechanisms should underlie the continuing decrease in macrophage disappearance from the lesions at the later time points, i.e. in the atherosclerosis regression phase. In this context, it is interesting to note that ApoE can facilitate anti-atherogenic cholesterol efflux [33,34]. It is therefore possible that ApoE secreted by newly infiltrated macrophages within the lesion might locally promote cholesterol efflux via ABCA1 (without intermediary involvement of HDL). However, it should be noted that the in vivo studies by Van Eck et al. have indicated that the change in serum cholesterol levels is the dominant factor in predicting the effect of ApoE on lesion development [34]. To explain the mechanism that underlies regression, it is important to take our findings regarding the effect of probucol treatment on atherosclerotic lesion regression into account. Probucol treatment on top of ApoE re-introduction was associated with functional HDL deficiency, a more pro-inflammatory / infiltrating (CCR2+) blood monocyte phenotype, decreased steroidogenesis and an apparent resistance to atherosclerosis regression. The observed shift in monocyte phenotype towards a more infiltrating subtype may also have contributed to the impairment of the regressive capacity of the lesions in probucol-treated mice. In support, Rahman et al. showed that progressive lesions have the blood signature of a pro-inflammatory monocyte phenotype, while the conversion towards anti-inflammatory monocyte is required to induce regression of lesions [35]. However, previous studies by the group of Ed Fisher have suggested that plasma HDL deficiency alone is already sufficient to disrupt the lesion regression capacity. They showed that transplantation

of an atherosclerotic lesion-rich aorta from hypercholesterolemic ApoE knockout mice into wild-type mice resulted in a rapid disappearance of lesional macrophages [36], an effect that was largely diminished when aortas were transplanted into HDL deficient ApoA1 knockout mice [14].

Further studies by Feig et al. have suggested that HDL, through lowering the cellular lipid content, increases the expression of the chemokine receptor CCR7 that facilitates macrophage emigration [14]. Given that blockade of CCR7 function significantly impairs the ability of macrophages to migrate out of the lesion, limiting the lesion regression potential in the aorta transplantation model [7], we highly likely assume that the functional HDL deficiency is the primary underlying cause of the detrimental effect of probucol treatment on lesion regression. Although we cannot exclude that besides the HDL lowering effect of probucol, additional probucol associated anti-oxidative mechanisms affect the lesion development. Additional studies will be needed to provide proof for the involvement of CCR7 in the effect of HDL on atherosclerosis regression in our current experimental regression mouse model.

Our recently established bone marrow transplantation-based atherosclerosis regression mouse model supplements the aforementioned aorta transplantation-based, Reversa, and ApoE adenovirus-based regression models first generated by respectively the groups of Ed Fisher [38, 36] Steve Young [37] and Dan Rader [10]. The current study highlights that (1) the absence of HDL in the plasma compartment limits the atherosclerosis regression potential in at least two out of 4 of the experimental models and (2) that this effect is not dependent on the exact cause of the HDL deficiency, i.e. genetic ablation of apolipoprotein A1 function versus pharmacological disruption of HDL lipidation through probucol treatment. Intriguingly, probucol treatment has been shown to increase the rate of reverse cholesterol transport [38], which should theoretically enhance the regression capacity. However, the effect of probucol on reverse cholesterol transport described by Yamamoto et al. [38] appears to be mainly driven by effects locally within the liver and not at the level of the macrophages. As such, we anticipate that increasing HDL-mediated cholesterol efflux through pharmacologically stimulating specifically the expression of the cellular cholesterol transport proteins interacting with HDL, i.e. ABCA1, ABCG1 and SR-BI, in macrophages is of clear therapeutic interest in the context of atherosclerosis regression. In further support of this notion, we have previously already shown that liver X receptor-mediated induction of ABCA1 and ABCG1 expression increases the ability of macrophages to disappear from established atherosclerotic lesions in our regression mouse model

[13]. Although we assume that ABCA1 should be considered the primary therapeutic target given its crucial role in the protection against macrophage foam cell formation and atherogenesis [39], additional mechanistic studies in the three regression mouse models are warranted to show the exact impact of the individual gene products involved in macrophage cholesterol efflux on atherosclerosis regression.

In conclusion, we have shown that probucol-induced HDL deficiency impairs the ability of established lesions to regress in response to reversal of the genetic hypercholesterolemia in ApoE knockout mice. Our studies thus highlight a crucial role for HDL in the process of atherosclerosis regression.

REFERENCES

1. Pagidipati, N. J. & Gaziano, T. A. Estimating deaths from cardiovascular disease: a review of global methodologies of mortality measurement. *Circulation* 127, 749-56 (2013).
2. Stegman, B. et al. Coronary atheroma progression rates in men and women following high-intensity statin therapy: A pooled analysis of REVERSAL, ASTEROID and SATURN. *Atherosclerosis* 254, 78-84 (2016).
3. Elshazly, M. B., Stegman, B. & Puri, R. Regression of coronary atheroma with statin therapy. *Curr. Opin. Endocrinol. Diabetes. Obes.* 23, 131-7 (2016).
4. Gragnano, F. & Calabrò, P. Role of dual lipid-lowering therapy in coronary atherosclerosis regression: Evidence from recent studies. *Atherosclerosis* 269, 219-228 (2018).
5. Feig, J. E. Regression of atherosclerosis: insights from animal and clinical studies. *Ann. Glob. Heal.* 80, 13-23 (2014).
6. Chereshnev, I. et al. Mouse model of heterotopic aortic arch transplantation. *J. Surg. Res.* 111, 171-6 (2003).
7. Trogan, E. et al. Gene expression changes in foam cells and the role of chemokine receptor CCR7 during atherosclerosis regression in ApoE-deficient mice. *Proc. Natl. Acad. Sci. U. S. A.* 103, 3781-6 (2006).
8. Feig, J. E. et al. Reversal of hyperlipidemia with a genetic switch favorably affects the content and inflammatory state of macrophages in atherosclerotic plaques. *Circulation* 123, 989-98 (2011).
9. Potteaux, S. et al. Suppressed monocyte recruitment drives macrophage removal from atherosclerotic plaques of ApoE-/- mice during disease regression. *J. Clin. Invest.* 121, 2025-2036 (2011).
10. Tsukamoto, K., Tangirala, R., Chun, S. H., Puré, E. & Rader, D. J. Rapid regression of atherosclerosis induced by liver-directed gene transfer of ApoE in ApoE-deficient mice. *Arterioscler. Thromb. Vasc. Biol.* 19, 2162-70 (1999).
11. Harris, J. D. et al. Acute regression of advanced and retardation of early aortic atheroma in immunocompetent apolipoprotein-E (apoE) deficient mice by administration of a second generation [E1(-), E3(-), polymerase(-)] adenovirus vector expressing human apoE. *Hum. Mol. Genet.* 11, 43-58 (2002).
12. Desurmont, C. et al. Complete atherosclerosis regression after human ApoE gene transfer in ApoE-deficient/nude mice. *Arterioscler. Thromb. Vasc. Biol.* 20, 435-42 (2000).
13. van der Stoep, M. et al. Elimination of macrophages drives LXR-induced regression both in initial and advanced stages of atherosclerotic lesion development. *Biochem. Pharmacol.* 86, 1594-602 (2013).
14. Feig, J. E. et al. HDL promotes rapid atherosclerosis regression in mice and alters inflammatory properties of plaque monocyte-derived cells. *Proc. Natl. Acad. Sci. U. S. A.* 108, 7166-71 (2011).
15. Feig, J. E., Hewing, B., Smith, J. D., Hazen, S. L. & Fisher, E. A. High-Density Lipoprotein and Atherosclerosis Regression. *Circ. Res.* 114, 205-213 (2014).
16. Hoekstra, M., Kruijt, J. K., Van Eck, M. & Van Berkel, T. J. C. Specific gene expression of ATP-binding cassette transporters and nuclear hormone receptors in rat liver parenchymal, endothelial, and Kupffer cells. *J. Biol. Chem.* 278, 25448-53 (2003).
17. van der Sluis, R. J., Nahon, J. E., Reuwer, A. Q., Van Eck, M. & Hoekstra, M. Haloperidol inhibits the development of atherosclerotic lesions in LDL receptor knockout mice. *Br. J. Pharmacol.* 172, 2397-405 (2015).
18. Van Eck, M. et al. Bone Marrow Transplantation in Apolipoprotein E Deficient Mice : Effect of ApoE Gene Dosage on Serum Lipid Concentrations, (beta)VLDL Catabolism, and Atherosclerosis. *Arterioscler. Thromb. Vasc. Biol.* 17, 3117-3126 (1997).
19. Champy, M.-F. et al. Genetic background determines metabolic phenotypes in the mouse. *Mamm. Genome* 19, 318-331 (2008).

20. Johnsen, S. H. et al. Monocyte count is a predictor of novel plaque formation: a 7-year follow-up study of 2610 persons without carotid plaque at baseline the Tromsø Study. *Stroke* 36, 715-9 (2005).
21. Adorni, M. P. et al. The roles of different pathways in the release of cholesterol from macrophages. *J. Lipid Res.* 48, 2453-62 (2007).
22. Wu, C.-A., Tsujita, M., Hayashi, M. & Yokoyama, S. Probucol inactivates ABCA1 in the plasma membrane with respect to its mediation of apolipoprotein binding and high density lipoprotein assembly and to its proteolytic degradation. *J. Biol. Chem.* 279, 30168-74 (2004).
23. Favari, E. et al. Probucol inhibits ABCA1-mediated cellular lipid efflux. *Arterioscler. Thromb. Vasc. Biol.* 24, 2345-50 (2004).
24. Tsujita, M., Tomimoto, S., Okumura-Noji, K., Okazaki, M. & Yokoyama, S. Apolipoprotein-mediated cellular cholesterol/phospholipid efflux and plasma high density lipoprotein level in mice. *Biochim. Biophys. Acta - Mol. Cell Biol. Lipids* 1485, 199-213 (2000).
25. Tomimoto, S. et al. Effect of probucol in lecithin-cholesterol acyltransferase-deficient mice: inhibition of 2 independent cellular cholesterol-releasing pathways in vivo. *Arterioscler. Thromb. Vasc. Biol.* 21, 394-400 (2001).
26. Hoekstra, M. et al. Plasma lipoproteins are required for both basal and stress-induced adrenal glucocorticoid synthesis and protection against endotoxemia in mice. *Am. J. Physiol. Endocrinol. Metab.* 299, E1038-E1043 (2010).
27. Hoekstra, M. et al. Scavenger receptor class B type I-mediated uptake of serum cholesterol is essential for optimal adrenal glucocorticoid production. *J. Lipid Res.* 50, 1039-1046 (2009).
28. Krinsky, N. I. The antioxidant and biological properties of the carotenoids. *Ann. N. Y. Acad. Sci.* 854, 443-7 (1998).
29. Zhang, Y. et al. Adipocyte modulation of high-density lipoprotein cholesterol. *Circulation* 121, 1347-55 (2010).
30. Han, K. H., Han, K. O., Green, S. R. & Quehenberger, O. Expression of the monocyte chemoattractant protein-1 receptor CCR2 is increased in hypercholesterolemia. Differential effects of plasma lipoproteins on monocyte function. *J. Lipid Res.* 40, 1053-63 (1999).
31. Swirski, F. K. et al. Identification of splenic reservoir monocytes and their deployment to inflammatory sites. *Science* 325, 612-6 (2009).
32. Lorimore, S. A., Coates, P. J., Scobie, G. E., Milne, G. & Wright, E. G. Inflammatory-type responses after exposure to ionizing radiation in vivo: a mechanism for radiation-induced bystander effects? *Oncogene* 20, 7085-95 (2001).
33. Bellosta, S. et al. Macrophage-specific expression of human apolipoprotein E reduces atherosclerosis in hypercholesterolemic apolipoprotein E-null mice. *J. Clin. Invest.* 96, 2170-9 (1995).
34. Van Eck, M. et al. Accelerated atherosclerosis in C57Bl/6 mice transplanted with ApoE-deficient bone marrow. *Atherosclerosis* 150, 71-80 (2000).
35. Rahman, K. et al. Inflammatory Ly6Chi monocytes and their conversion to M2 macrophages drive atherosclerosis regression. *J. Clin. Invest.* 127, 2904-2915 (2017).
36. Reis, E. D. et al. Dramatic remodeling of advanced atherosclerotic plaques of the apolipoprotein E-deficient mouse in a novel transplantation model. *J. Vasc. Surg.* 34, 541-7 (2001).
37. Lieu, H. D. et al. Eliminating atherogenesis in mice by switching off hepatic lipoprotein secretion. *Circulation* 107, 1315-21 (2003).
38. Yamamoto, S. et al. Pharmacologic Suppression of Hepatic ATP-Binding Cassette Transporter 1 Activity in Mice Reduces High-Density Lipoprotein Cholesterol Levels but Promotes Reverse Cholesterol Transport. *Circulation* 124, 1382-1390 (2011).
39. Singaraja, R. R. et al. Increased ABCA1 activity protects against atherosclerosis. *J. Clin. Invest.* 110, 35-42 (2002).

3

Division of BioTherapeutics, Leiden Academic Centre for Drug Research,
Leiden, The Netherlands

BBA - Molecular and Cell Biology of Lipids 1865:7 158682 (2020)